

Electronic Supplementary Information (ESI)

Artificial Neural Network Encoding of Molecular Wave Function for Quantum Computing

Masaya Hagai,^{*,†} Mahito Sugiyama,[‡] Koji Tsuda,^{¶§,⊥} and Takeshi Yanai^{*,||,†}

[†]*Department of Chemistry, Nagoya University, Furocho, Chikusa Ward, Nagoya, Aichi 464-8601, Japan*

[‡]*National Institute of Informatics, 2-1-2 Hitotsubashi, Chiyoda-ku, Tokyo 101-8430, Japan*

[¶]*Graduate School of Frontier Sciences, The University of Tokyo, 5-1-5 Kashiwa-no-ha, Kashiwa, Chiba 277-8561, Japan*

[§]*RIKEN Center for Advanced Intelligence Project, 1-4-1 Nihonbashi, Chuo-ku, Tokyo 103-0027, Japan*

^{||}*Institute of Transformative Bio-Molecules (WPI-ITbM), Nagoya University, Furocho, Chikusa Ward, Nagoya, Aichi 464-8601, Japan*

[⊥]*Research and Services Division of Materials Data and Integrated System, National Institute for Materials Science, Ibaraki 305-0047, Japan*

E-mail: hagai.masaya.v9@s.mail.nagoya-u.ac.jp; yanait@chem.nagoya-u.ac.jp

Contents

S1 Algorithms and Theory	3
S1.1 Quantum Phase Estimation (QPE) Based Energy Function Evaluation	3
S1.2 Energy Curation Gate To Evaluate Converted BM2 Energy Function	4
S1.3 Phase preparation with BM2 model	5
S1.4 Quantum Amplitude Amplification	6
S1.5 Preparation of Particle-Number Conserving Initial State for CAS(4e,4o) of Singlet State	7
S1.6 Calculation of Energy and Its Gradients	8
S1.7 Prototyping on Quantum Computer Simulator	11
S1.8 Additional Background of This Work	12
S2 Benchmark Data	13
S2.1 PECs of H ₂ with BM2(FS), BM3(FS), and RBM(FS)	13
S2.2 PECs of H ₂ with BM2(PN), BM3(PN)	16
S2.3 s-trans and s-cis butadiene with BM2(FS), BM3(FS), and RBM(FS)	18
S2.4 PECs of PABI with BM2(PN) and BM3(PN)	19
S2.5 LMOs used in the calculation for PABI	19
S2.6 Configuration weights for PABI	20
References	21

S1 Algorithms and Theory

S1.1 Quantum Phase Estimation (QPE) Based Energy Function Evaluation

[Algorithm S1](#) is used as an intermediate process or subroutine of [Algorithm 1](#) (see also Sec. 2.2.2). The purpose of [Algorithm S1](#) is transforming $\frac{1}{\sqrt{2^{n_v}}} \sum_{\mathbf{v}} |\mathbf{v}\rangle |0\rangle_{n_{\text{reg}}}$ (input object) into $\frac{1}{\sqrt{2^{n_v}}} \sum_{\mathbf{v}} |\mathbf{v}\rangle |\tilde{\mathbf{E}}_{\mathbf{v}}\rangle_{n_{\text{reg}}}$ (output object). This means that the values of the converted BM energy function $\tilde{E}_{\mathbf{v}}$ ([eq. \(9\)](#)) are stored onto the energy register qubits. This process is based on Kitaev's QPE algorithm,¹ which allows ones to find the phase (i.e., $\tilde{E}_{\mathbf{v}}$ in this algorithm) of the eigenvalue for the given unitary operator U .

The operator object U or its quantum circuit needs to be given as another input to [Algorithm S1](#). The unitary operator U is constructed based on the condition that the bitstring \mathbf{v} and associated phase $e^{2\pi i \tilde{E}_{\mathbf{v}}}$ are its eigenvector and eigenvalue, respectively; i.e., $U |\mathbf{v}\rangle = e^{2\pi i \tilde{E}_{\mathbf{v}}} |\mathbf{v}\rangle$. At the core of [Algorithm S1](#), the bitwise transformations are subsequently performed to register the bit information of $\tilde{E}_{\mathbf{v}}$ on the energy register qubits using the inputed U , as just done in Kitaev's QPE algorithm. The operator U here serves as a lower-level subroutine. Its programmable procedure is described in detail in [Algorithm S2](#).

Algorithm S1 Energy function evaluation based on quantum phase estimation (QPE) algorithm. The values of the converted energy function \tilde{E} are efficiently recorded onto the register qubits in the superposition state.

Input:

- Energy curation gate: $U(\sum_{\mathbf{v}} C_{\mathbf{v}} |\mathbf{v}\rangle) = \sum_{\mathbf{v}} C_{\mathbf{v}} e^{2\pi i \tilde{E}_{\mathbf{v}}} |\mathbf{v}\rangle$
 - The gate U is described in [Algorithm S2](#).
- Quantum state: $|\Psi_{\text{in}}\rangle = \frac{1}{\sqrt{2^{n_v}}} \sum_{\mathbf{v}} |\mathbf{v}\rangle |0\rangle_{n_{\text{reg}}}$

Output:

- Quantum state: $|\Psi_{\text{out}}\rangle = \frac{1}{\sqrt{2^{n_v}}} \sum_{\mathbf{v}} |\mathbf{v}\rangle |\tilde{\mathbf{E}}_{\mathbf{v}}\rangle_{n_{\text{reg}}}$
 - $|\tilde{\mathbf{E}}_{\mathbf{v}}\rangle_{n_{\text{reg}}}$ is an n_{reg} -bit representation of $\tilde{E}_{\mathbf{v}}$.

Procedure

for $i = 1 \dots n_{\text{reg}}$ **do**

 Apply the Hadamard gate on i -th energy register qubit.

$$\triangleright |\Psi_{\text{in}}\rangle \equiv \frac{1}{\sqrt{2^{n_v}}} \sum_{\mathbf{v}} |\mathbf{v}\rangle |0\rangle_{n_{\text{reg}}} \rightarrow \frac{1}{\sqrt{2^{n_v+n_{\text{reg}}}}} \sum_{\mathbf{v}} \sum_{k=0}^{2^{n_{\text{reg}}}-1} |\mathbf{v}\rangle |k\rangle$$

end for

for $i = 1 \dots n_{\text{reg}}$ **do**

 Apply the energy curation gate $U^{2^{i-1}}$ on $|\Psi\rangle$ controlled on i -th energy register qubit.

$$\triangleright |\Psi\rangle \rightarrow \frac{1}{\sqrt{2^{n_v+n_{\text{reg}}}}} \sum_{\mathbf{v}} \sum_{k=0}^{2^{n_{\text{reg}}}-1} e^{2\pi i k \tilde{E}_{\mathbf{v}}} |\mathbf{v}\rangle |k\rangle$$

end for

Perform the inverse quantum Fourier transformation (inverse QFT) on the register qubits.

$$\triangleright |\Psi\rangle \rightarrow \frac{1}{\sqrt{2^{n_v}}} \sum_{\mathbf{v}} |\mathbf{v}\rangle |\tilde{\mathbf{E}}_{\mathbf{v}}\rangle_{n_{\text{reg}}} \equiv |\Psi_{\text{out}}\rangle$$

end Procedure

S1.2 Energy Curation Gate To Evaluate Converted BM2 Energy Function

As written Sec. S1.1 and also Sec. 2.2.2, we need to develop the unitary operator U that transforms the bitstring state $|\mathbf{v}\rangle$ to the scaled state $e^{2\pi i \tilde{E}_{\mathbf{v}}} |\mathbf{v}\rangle$. The quantum algorithm for achieving this objective is given in [Algorithm S2](#). The converted energy function \tilde{E} is defined in [eq. \(9\)](#) based on the parameters θ , D , and Δ , which are given as inputs. [Algorithm S2](#) is used as a subroutine of [Algorithm S1](#). This unitary gate is named the energy curation gate. As shown in [Algorithm S2](#), the quantum circuit acting as U is constructed mainly using the phase shift rotation $R'_z(\theta)$ gates. [Algorithm S2](#) is the gate for the BM2 energy function; however, one can easily extend this algorithm to BM3 and RBM energy functions by adding the phase shift rotation gates or modifying the loop indices.

Algorithm S2 Energy curation gate attaching the values of converted BM2 energy function $\tilde{E}_{\mathbf{v}}(\theta)$. This gate serves as a subroutine in the QPE based procedure ([Algorithm S1](#)).

Input:

- Model parameters: θ ($= \{a_i\} \oplus \{w_{ij}\}$)
- Scaling constant: D
- Shifting constant: Δ
- Quantum state: $|\Psi_{\text{in}}\rangle = \sum_{\mathbf{v}} C_{\mathbf{v}} |\mathbf{v}\rangle$

Output:

- Quantum state: $|\Psi_{\text{out}}\rangle = \sum_{\mathbf{v}} C_{\mathbf{v}} e^{2\pi i \tilde{E}_{\mathbf{v}}(\theta)} |\mathbf{v}\rangle$

Procedure

for $i = 1 \dots n_v$ **do**

 Apply the phase shift rotation $R'_z(2\pi a_i/D)$ gate on i -th visible qubit.

$$\triangleright |\Psi_{\text{in}}\rangle \equiv \sum_{\mathbf{v}} C_{\mathbf{v}} |\mathbf{v}\rangle \rightarrow \sum_{\mathbf{v}} C_{\mathbf{v}} e^{2\pi i (\sum_i^n a_i v_i)/D} |\mathbf{v}\rangle$$

end for

for $i = 1 \dots n_v$ **do**

for $j = 1 \dots n_v$ **do**

if $i = j$ **then**

 Apply the phase shift rotation $R'_z(2\pi w_{ii}/D)$ gate on i -th visible qubit.

else

 Apply the phase shift rotation $R'_z(2\pi w_{ij}/D)$ gate on i -th visible qubit conditioned on j -th visible qubit.

end if

$$\triangleright |\Psi\rangle \rightarrow \sum_{\mathbf{v}} C_{\mathbf{v}} e^{2\pi i (\sum_i^n a_i v_i + \sum_{ij}^n w_{ij} v_i v_j)/D} |\mathbf{v}\rangle$$

end for

end for

 Apply the identity operator $R_I(2\pi \Delta)$ gate on the first visible qubit. (This process can be omitted.)

$$\triangleright |\Psi\rangle \rightarrow \sum_{\mathbf{v}} C_{\mathbf{v}} e^{2\pi i ((\sum_i^n a_i v_i + \sum_{ij}^n w_{ij} v_i v_j)/D + \Delta)} |\mathbf{v}\rangle = \sum_{\mathbf{v}} C_{\mathbf{v}} e^{2\pi i \tilde{E}_{\mathbf{v}}(\theta)} |\mathbf{v}\rangle \equiv |\Psi_{\text{out}}\rangle$$

end Procedure

- This algorithm can be readily extended to the energy functions of the BM3 and RBM models.
- The phase shift rotation $R'_z(\theta)$ is defined in [eq. \(10\)](#) in the main text.
- The identity operator $R_I(\theta)$ is defined by

$$R_I(\theta) = \begin{pmatrix} e^{i\theta} & 0 \\ 0 & e^{i\theta} \end{pmatrix} \quad (\text{S1})$$

- $\tilde{E}_{\mathbf{v}}(\theta)$ is the converted BM2 energy function, given as $\tilde{E}_{\mathbf{v}}(\theta) = E^{\text{BM2}}(\mathbf{v}; \theta)/D + \Delta$.

S1.3 Phase preparation with BM2 model

The purpose of [Algorithm S3](#) is augmenting $\sum_v C_v |v\rangle$ (input object) with the phase factor $e^{\frac{i}{2}E^{\text{BM2}}(v;\tau)}$ to yield the superposition state $\sum_v C_v e^{\frac{i}{2}E^{\text{BM2}}(v;\tau)} |v\rangle$ (output object). See also Sec. 2.2.3 and [Algorithm 1](#). The parameters τ of the phase factor serve as input parameters. The quantum circuit of [Algorithm S3](#) is composed of the phase shift rotation $R'_z(\theta)$ gates.

Algorithm S3 Phase preparation with BM2 model

Input:

- Model parameters: $\tau (= \{c_i\} \oplus \{x_{ij}\})$
- Quantum state: $|\Psi_{\text{in}}\rangle = \sum_v C_v |v\rangle$

Output:

- Quantum state: $|\Psi_{\text{out}}\rangle = \sum_v C_v e^{\frac{i}{2}E^{\text{BM2}}(v;\tau)} |v\rangle$

Procedure
for $i = 1 \dots n_v$ **do**

 Apply the phase shift rotation $R'_z(c_i/2)$ gate on i -th visible qubit.

$$\triangleright |\Psi_{\text{in}}\rangle \equiv \sum_v C_v |v\rangle \rightarrow \sum_v C_v e^{\frac{i}{2}(\sum_i^n c_i v_i)} |v\rangle$$

end for
for $i = 1 \dots n_v$ **do**
for $j = 1 \dots n_v$ **do**
if $i = j$ **then**

 Apply the phase shift rotation $R'_z(x_{ii}/2)$ gate on i -th visible qubit.

else

 Apply the phase shift rotation $R'_z(x_{ij}/2)$ gate on i -th visible qubit conditioned on j -th visible qubit.

end if

$$\triangleright |\Psi\rangle \rightarrow \sum_v C_v e^{\frac{i}{2}(\sum_i^n c_i v_i + \sum_{ij}^{n_v} x_{ij} v_i v_j)} |v\rangle = \sum_v C_v e^{\frac{i}{2}E^{\text{BM2}}(v;\tau)} |v\rangle \equiv |\Psi_{\text{out}}\rangle$$

end for
end for
end Procedure

- This algorithm can be readily extended to the energy functions of the BM3 and RBM models.
- Algorithm [S3](#) bears a close resemblance to Algorithm [S2](#).
- The phase shift rotation $R'_z(\theta)$ is defined in eq. (10) in the main text.

S1.4 Quantum Amplitude Amplification

To maximize the probability of observing the ancilla qubits to be $|0\rangle_{n_{\text{reg}}}$ as written in Algorithm 1, we use the quantum amplitude amplification.² This process enables a quadratic increase in the probability of finding the target state. The flow of the algorithm is sketched as follows.

Algorithm S4 Quantum amplitude amplification

Input:

- Number of iterations: N
- Quantum State: $|\Psi_{\text{in}}\rangle = \sin(\theta) |\Phi\rangle |0\rangle_{n_{\text{reg}}} + \dots$

Output:

- Quantum State: $|\Psi_{\text{out}}\rangle = \sin((2N+1)\theta) |\Phi\rangle |0\rangle_{n_{\text{reg}}} + \dots$

Procedure

```

for  $k = 1 \dots N$  do
    Apply the reflection gate  $U_w$  (eq. (S2)) on the energy register bits with  $|0\rangle_{n_{\text{reg}}}$ .
    Apply the reflection gate  $U_s$  (eq. (S4)) on the state  $|\Phi\rangle |0\rangle_{n_{\text{reg}}}$ .
     $\triangleright |\Psi_1\rangle \equiv |\Psi_{\text{in}}\rangle$ 
     $\triangleright |\Psi_k\rangle = \sin((2(k-1)+1)\theta) |\Phi\rangle |0\rangle_{n_{\text{reg}}} + \dots$ 
     $\rightarrow |\Psi_{k+1}\rangle = \sin((2k+1)\theta) |\Phi\rangle |0\rangle_{n_{\text{reg}}} + \dots$ 
end for
 $\triangleright |\Psi_{N+1}\rangle \equiv |\Psi_{\text{out}}\rangle$ 
end Procedure

```

- The reflection gate U_w is given by

$$U_w = I - 2|0\rangle_{n_{\text{reg}}} \langle 0|_{n_{\text{reg}}}. \quad (\text{S2})$$

It acts as a reflection of the given $|\Psi\rangle$ across the ancilla bits $|\mathbf{k}\rangle_{n_{\text{reg}}}$, making an inversion controlled by the state of $|\mathbf{k}\rangle_{n_{\text{reg}}}$. Applying U_w onto $|\mathbf{k}\rangle_{n_{\text{reg}}}$ yields

$$U_w |\mathbf{k}\rangle_{n_{\text{reg}}} = \begin{cases} -|\mathbf{k}\rangle_{n_{\text{reg}}} & (\mathbf{k} = \mathbf{0}) \\ |\mathbf{k}\rangle_{n_{\text{reg}}} & (\mathbf{k} \neq \mathbf{0}) \end{cases}. \quad (\text{S3})$$

- The additional reflection gate U_s leads to a further reflection around the state $|\Phi\rangle |0\rangle_{n_{\text{reg}}}$, which is the state whose probability we want to raise.

$$\begin{aligned} U_s &= 2|\Phi\rangle |0\rangle_{n_{\text{reg}}} \langle 0|_{n_{\text{reg}}} \langle \Phi| - I \\ &= 2S|0\rangle |0\rangle_{n_{\text{reg}}} \langle 0|_{n_{\text{reg}}} \langle 0| S^\dagger - I \\ &= -SS_0S^\dagger \end{aligned} \quad (\text{S4})$$

where S and S_0 are defined as

$$S|0\rangle = |\Phi\rangle, \quad (\text{S5})$$

and

$$S_0 = I - 2|0\rangle |0\rangle_{n_{\text{reg}}} \langle 0|_{n_{\text{reg}}} \langle 0|, \quad (\text{S6})$$

respectively.

- These two reflection gates U_w and U_s are applied alternately, increasingly enlarging the probability of finding state $|0\rangle_{n_{\text{reg}}}$ in a quadratical rate.

S1.5 Preparation of Particle-Number Conserving Initial State for CAS(4e,4o) of Singlet State

On the basis of Ref. 3, we use the following quantum circuit $U_{\text{PN}} |0000\rangle$ depicted in Figure S1 for the preparation of a particle-number (PN) conserving state for the singlet-state CAS(4e,4o) calculation.

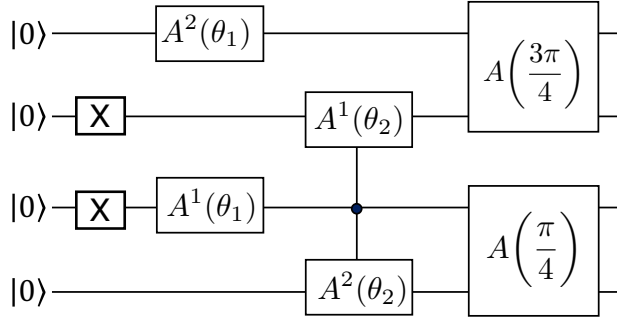


Figure S1: Quantum circuit representing $U_{\text{PN}} |0000\rangle$, yielding a particle-number (PN) conserving state for the singlet-state CAS(4e,4o). $\theta_1 = \arcsin(\sqrt{1/6})$ and $\theta_2 = \arcsin(\sqrt{1/5})$.

This quantum circuit U_{PN} is built from the two-qubit operator $A(\theta)$, which is defined as follows,

$$A(\theta) = \begin{pmatrix} 1 & 0 & 0 & 0 \\ 0 & \cos(\theta) & \sin(\theta) & 0 \\ 0 & \sin(\theta) & -\cos(\theta) & 0 \\ 0 & 0 & 0 & 1 \end{pmatrix}. \quad (\text{S7})$$

Applying U_{PN} on the zero state $|0000\rangle$ results in the state preparation of an equally-weighted superposition of all the particle-number (PN) conserving bitstrings, which are six in total, as follows:

$$U_{\text{PN}} |0000\rangle = \frac{1}{\sqrt{6}}(|1100\rangle + |1010\rangle + |1001\rangle + |0110\rangle + |0101\rangle + |0011\rangle). \quad (\text{S8})$$

As written in the main text, the initial state prepared with Fock space (FS) treatment is formed by applying the Hadamard gate based circuit, here denoted U_{FS} , on $|0000\rangle$, as follows:

$$\begin{aligned} U_{\text{FS}} |0000\rangle = & \frac{1}{4}(|0000\rangle + |0001\rangle + |0010\rangle + |0011\rangle \\ & + |0100\rangle + |0101\rangle + |0110\rangle + |0111\rangle \\ & + |1000\rangle + |1001\rangle + |1010\rangle + |1011\rangle \\ & + |1100\rangle + |1101\rangle + |1110\rangle + |1111\rangle), \end{aligned} \quad (\text{S9})$$

which consists of sixteen bitstrings.

S1.6 Calculation of Energy and Its Gradients

The CAS-CI theory is based on the second-quantized form of the *active-space* Hamiltonian written as

$$\hat{H} = H_0 + \sum_{pq}^K (p|\hat{h}|q) \hat{E}_{pq} + \frac{1}{2} \sum_{pqrs}^K (pq|rs)(\hat{E}_{pq}\hat{E}_{rs} - \delta_{qr}\hat{E}_{ps}), \quad (\text{S10})$$

where K is the number of the spatial orbitals treated as the active orbitals. The so-called generator \hat{E}_{pq} , often used in the formulation of the multiconfigurational or multireference methods, is given as

$$\hat{E}_{pq} = \hat{a}_{p\alpha}^\dagger \hat{a}_{q\alpha} + \hat{a}_{p\beta}^\dagger \hat{a}_{q\beta}. \quad (\text{S11})$$

with $\hat{a}_{p\alpha}^\dagger$ ($\hat{a}_{p\alpha}$) is the fermionic creation (annihilation) operator associated with the α -spin electron in the p -th spatial orbital. The coefficients $(p|\hat{h}|q)$ and $(pq|rs)$ in eq. (S10) are one-electron and two-electron integrals, respectively, the values of which are offered by standard quantum chemistry programs, along with a constant H_0 that accounts for the nuclear repulsion energy and close-shell electron energy (see also Ref. 4 for detail).

The Hamiltonian (eq. (S10)) is converted by the Jordan-Wigner (JW) encoding into the expression using Pauli operators in a form suited for the quantum simulation of electronic structure on a quantum computer. As shown in the review articles,^{5–10} this conversion is carried out by the qubit mapping of the creation and annihilation operators into the Pauli operators X_p , Y_p , Z_p , and I_p as given by

$$\hat{a}_p^\dagger = \frac{1}{2}(X_p - iY_p) \otimes Z_{p-1} \otimes Z_{p-2} \otimes \dots \otimes Z_0, \quad (\text{S12})$$

$$\hat{a}_p = \frac{1}{2}(X_p + iY_p) \otimes Z_{p-1} \otimes Z_{p-2} \otimes \dots \otimes Z_0. \quad (\text{S13})$$

The insertion of eqs. (S12) and (S13) into the Hamiltonian (eq. (S10)) results in the JW-transformed Hamiltonian written as,

$$\hat{H} = h_0 + \sum_{i\alpha} h_\alpha^i \sigma_\alpha^i + \sum_{ij\alpha\beta} h_{\alpha\beta}^{ij} \sigma_\alpha^i \sigma_\beta^j + \dots \quad (\text{S14})$$

forming a linear combination of single-qubit Pauli operators denoted $\sigma_\alpha^i \in \{I_i, X_i, Y_i, Z_i\}$. The coefficients h_α^i , $h_{\alpha\beta}^{ij}$, \dots are real-scalar constants that originate from the one- and two-electron integrals of eq. (S10).

In our BM/RBM based NQS calculation, the learning parameters of the wave function $|\Psi\rangle$ are determined in a spirit similar to the reinforce learning by minimizing the total energy, which is given as the expectation of the Hamiltonian $\langle \hat{H} \rangle \equiv \langle \Psi | \hat{H} | \Psi \rangle$. The methods to evaluate $\langle \hat{H} \rangle$ on a quantum computer have been deeply studied in the context of the development of the VQE framework. The computation of $\langle \hat{H} \rangle$ based on JW-transformed Hamiltonian (eq. (S14)) reduces to the sum of a polynomial number of expectation values of the Pauli operators for $|\Psi\rangle$, as follows,

$$E = \langle \hat{H} \rangle = h_0 + \sum_{i\alpha} h_\alpha^i \langle \sigma_\alpha^i \rangle + \sum_{ij\alpha\beta} h_{\alpha\beta}^{ij} \langle \sigma_\alpha^i \sigma_\beta^j \rangle + \dots. \quad (\text{S15})$$

In the scheme designated *Hamiltonian averaging*, eq. (S15), namely $\langle \hat{H} \rangle$ in the JW-transformed form, can be efficiently estimated on a quantum computer with the prepared $|\Psi\rangle$. On the basis of this scheme, the present NQS method as a quantum algorithm thus employs the JW transformation of the Hamiltonian (eq. (S14)) and evaluate the energy $\langle \hat{H} \rangle$ (eq. (S15)) with the NQS state updated in the training process.

As discussed in the main text, the training is carried out using the gradients of the energy with respect to the

learning parameters σ ($\equiv (\theta, \tau)$), which are given as follows,

$$\begin{aligned}\frac{\partial E}{\partial \theta} &= 2\text{Re}[\langle HO^\theta \rangle - \langle H \rangle \langle O^\theta \rangle] \\ \frac{\partial E}{\partial \tau} &= 2\text{Re}[\langle HO^\tau \rangle - \langle H \rangle \langle O^\tau \rangle].\end{aligned}\quad (\text{S16})$$

Note the intermediate operator O_v^σ ($= \frac{\partial}{\partial \sigma} \log C_v$) is introduced in the main text (see also Ref. 4). Give that the BM2/BM3 parameter set contains θ ($= \{a_i\} \oplus \{w_{ij}\} \oplus \{w_{ijk}\}$) for the amplitude segment, the tangible expressions of the operators O_v^θ arising in the BM2/BM3 model are written as

$$\begin{aligned}O_{v'}^{a_i} &= \frac{1}{2}[v'_i - \langle v_i \rangle] &= \frac{1}{4}[(I_i - Z_i) - \langle I_i - Z_i \rangle], \\ O_{v'}^{w_{ij}} &= \frac{1}{2}[v'_i v'_j - \langle v_i v_j \rangle] &= \frac{1}{8}[(I_i - Z_i)(I_j - Z_j) - \langle (I_i - Z_i)(I_j - Z_j) \rangle], \\ O_{v'}^{w_{ijk}} &= \frac{1}{2}[v'_i v'_j v'_k - \langle v_i v_j v_k \rangle] &= \frac{1}{16}[(I_i - Z_i)(I_j - Z_j)(I_k - Z_k) - \langle (I_i - Z_i)(I_j - Z_j)(I_k - Z_k) \rangle].\end{aligned}\quad (\text{S17})$$

As this study models the phase segment commonly using the energy function with the BM2 parameters τ ($= \{c_i\} \oplus \{x_{ij}\}$), the associated operators O_v^τ are expressed as

$$\begin{aligned}O_{v'}^{c_i} &= \frac{i}{2}[v'_i] &= \frac{i}{4}[I_i - Z_i], \\ O_{v'}^{x_{ij}} &= \frac{i}{2}[v'_i v'_j] &= \frac{i}{8}[(I_i - Z_i)(I_j - Z_j)],\end{aligned}\quad (\text{S18})$$

The important finding in eqs. (S17) and (S18) is that the operators O_v^σ for BM2 and BM3 can all be expressed with the Pauli operators as well as their expectation values. Inserting eqs. (S17) and (S18) into eq. (S16), we reach the following working equations based on Pauli operators, which take suited form to evaluate the gradients on a quantum computer, as

$$\begin{aligned}\frac{\partial E}{\partial a_i} &= -\frac{1}{2}\text{Re}[\langle H Z_i \rangle - \langle H \rangle \langle Z_i \rangle], \\ \frac{\partial E}{\partial w_{ij}} &= -\frac{1}{4}\text{Re}[\langle H(Z_i + Z_j - Z_i Z_j) \rangle - \langle H \rangle \langle Z_i + Z_j - Z_i Z_j \rangle], \\ \frac{\partial E}{\partial w_{ijk}} &= -\frac{1}{8}\text{Re}[\langle H(Z_i + Z_j + Z_k - Z_i Z_j - Z_j Z_k - Z_k Z_i + Z_i Z_j Z_k) \rangle \\ &\quad - \langle H \rangle \langle Z_i + Z_j + Z_k - Z_i Z_j - Z_j Z_k - Z_k Z_i + Z_i Z_j Z_k \rangle],\end{aligned}\quad (\text{S19})$$

and

$$\begin{aligned}\frac{\partial E}{\partial c_i} &= \frac{1}{2}\text{Im}[\langle H Z_i \rangle - \langle H \rangle \langle Z_i \rangle], \\ \frac{\partial E}{\partial x_{ij}} &= \frac{1}{4}\text{Im}[\langle H(Z_i + Z_j - Z_i Z_j) \rangle - \langle H \rangle \langle Z_i + Z_j - Z_i Z_j \rangle].\end{aligned}\quad (\text{S20})$$

In a similar vein to the Hamiltonian averaging, all the expectation values in the gradients (eqs. (S19) and (S20)) can thus be calculated by a linear combination of the averages of the Pauli operator strings.

It should be stressed that the gradients for the RBM model do not have such favorable expressions to be straightforwardly implemented in the quantum circuit. For the amplitude segment in the RBM model, as shown in

the previous works, the operators O_v^θ are derived as

$$\begin{aligned} O_{v'}^{a_i} &= \frac{1}{2} \left[v'_i - \langle v_i \rangle \right], \\ O_{v'}^{b_j} &= \frac{1}{2} \left[\text{Sig} \left(b_j + \sum_I v'_I w_{Ij} \right) - \left\langle \text{Sig} \left(b_j + \sum_I v_I w_{Ij} \right) \right\rangle \right], \\ O_{v'}^{w_{ij}} &= \frac{1}{2} \left[v'_i \text{Sig} \left(b_j + \sum_I v'_I w_{Ij} \right) - \left\langle v_i \text{Sig} \left(b_j + \sum_I v_I w_{Ij} \right) \right\rangle \right], \end{aligned} \quad (\text{S21})$$

where $\text{Sig}(x)$ is the sigmoid function defined by $\text{Sig}(x) = \frac{e^x}{e^x + 1}$. The development of the algorithm to evaluate $\text{Sig}(x)$ on a quantum computer requires additional research. In this work based on the quantum computer simulator, the evaluation of the sigmoid function is replaced by the classical computation as if it could be computed on a quantum computer by a third-party subroutine, which is currently hypothetical.

On an additional note, we use a gradient-based method called the stochastic reconfiguration (SR) to update the learning parameters, as also employed in the previous works. The training undergoes the iterative correction to the parameters. The update at the n -th iteration is written as

$$\begin{aligned} \theta^{(n+1)} &= \theta^{(n)} - \alpha \sum_{\theta'} \mathbf{S}_{\theta\theta'}^{-1} \mathbf{F}_\theta, \\ \tau^{(n+1)} &= \tau^{(n)} - \alpha \sum_{\tau'} \mathbf{S}_{\tau\tau'}^{-1} \mathbf{F}_\tau. \end{aligned} \quad (\text{S22})$$

where \mathbf{F}_θ and \mathbf{F}_τ refer to the gradients of the energy with respect to the learning parameters θ and τ , respectively, corresponding to [eq. \(S19\)](#) and [eq. \(S20\)](#), respectively. The SR method uses the Hermitian covariance matrices $\mathbf{S}_{\theta\theta'}$ and $\mathbf{S}_{\tau\tau'}$ defined as

$$\begin{aligned} \mathbf{S}_{\theta\theta'} &= \text{Re} \left[\left\langle (O^\theta - \langle O^\theta \rangle)^* (O^{\theta'} - \langle O^{\theta'} \rangle) \right\rangle \right], \\ \mathbf{S}_{\tau\tau'} &= \text{Re} \left[\left\langle (O^\tau - \langle O^\tau \rangle)^* (O^{\tau'} - \langle O^{\tau'} \rangle) \right\rangle \right], \end{aligned} \quad (\text{S23})$$

serving as a kind of the preconditioner to bring improvement of the convergence to the minimized variational energy. [Equation \(S23\)](#) can be rewritten as

$$\begin{aligned} \mathbf{S}_{\theta\theta'} &= \text{Re} \left[\left\langle O^{\theta*} O^{\theta'} \right\rangle - \left\langle O^{\theta*} \right\rangle \left\langle O^{\theta'} \right\rangle \right], \\ \mathbf{S}_{\tau\tau'} &= \text{Re} \left[\left\langle O^{\tau*} O^{\tau'} \right\rangle - \left\langle O^{\tau*} \right\rangle \left\langle O^{\tau'} \right\rangle \right]. \end{aligned} \quad (\text{S24})$$

With the BM2 and BM3 models, these can be evaluated as a linear combination of the expectation values of the Pauli operator strings.

S1.7 Prototyping on Quantum Computer Simulator

Our hybrid quantum-classical algorithm was prototyped for determining the NQS was implemented into a Python-based computer code. See also the source code offered as part of ESI for details. The quantum computation procedures were programmed using classical emulation of elementary quantum gates and qubit operations implemented in the QC simulator QULACS.¹¹ The mapping of the fermionic molecular Hamiltonian H to the qubit representation with the Pauli matrices was done through the Jordan-Wigner transformation¹² using the quantum algorithm library OPENFERMION.¹³ We used its plugin to import the Hamiltonian's integrals in canonical and localized molecular orbital basis, which were offered by the electronic structure package PYSCF.¹⁴

Our implementation simulates the state preparation by manipulating entangled $(n_v + n_h + 2 \times n_{\text{reg}})$ qubits as formulated in Section 2. However, the simulator-based implementation faces a limitation in execution when increasing the number of the energy register qubits and ancilla qubits (Fig 2(a)), given as $2 \times n_{\text{reg}}$ in total. With n_{reg} set to ten or larger, we switch to a corner-cutting implementation that circumvents the explicit formation of these qubits and instead uses a separated data storage with the size of 2^{n_v} that keep the converted energy \tilde{E}_v with its n_{reg} -bit precision in high-speed memory. This simplification is possible because $|v\rangle$ and $|\tilde{E}_v\rangle$ are maximally entangled in the superposition, as shown in eq. (8). Moreover, the ancilla qubits can also be eliminated by directly replacing the quantum procedure of the Gibbs state formation (eq. (12)) with its classical computation that evaluates $\sqrt{e^E(v;\theta)}$ using Python's mathematical functions via access to the data array of \tilde{E}_v . We confirmed that this corner-cutting treatment certainly reproduces preciously the same numeric results as yielded by the full-fledged QC simulation, thus being confirmed to offer an exact emulation of the roles of the energy register and ancilla qubits. On an additional note, as discussed in Sec. 2, the gradients of the RBM-based NQS energy involves the sigmoid function, which cannot expressed with the Pauli strings; thus, on the simulator, we evaluated it classically.

Once the gradients are obtained, the training of the BM2, BM3, and RBM models was performed with the gradient based optimization. Its computation poses no more than classical complexity and can thus be carried out efficiently on a classical computer as done previously.⁴ Its implementation is essentially the same as developed in the previous work. To deal with highly nonlinear dependence on the learning parameters in the variational minimization, the training program can use the stochastic reconfiguration method,¹⁵ as done previously, and the quasi-Newton Raphson method, which are both considered to be capable of stably finding minima. Technical details of the optimization are described in Ref. 4.

S1.8 Additional Background of This Work

Tensor Network Theory: A light is shed on the neural network state (NQS) in the sense that it can be regarded as bearing an intimate relation to another class of quantum physical framework, designated tensor networks theory,¹⁶ including density matrix renormalization group (DMRG)^{17,18} or matrix product states (MPS),^{19,20} tree tensor networks (TTN),²¹ projected entangled pair state (PEPS),²² multi-scale entanglement renormalization (MERA),²³ and many others.¹⁶ The developments of these tensor networks explore effective factorizations of quantum entanglement into local objects correlated in certain dimensions.

Ab Initio Multireference Methods as CAS-CI Solver: Related to the NQS method used as CAS-CI solver, there are various algorithms developed to circumvent the exponentially-growing complexity of the multireference calculations, such as *ab initio* density matrix renormalization group,²⁴ full CI quantum Monte Carlo,²⁵ full coupled-cluster reduction,²⁶ many-body expanded full CI,²⁷ auxiliary-field quantum monte carlo,²⁸ variational two-electron reduced density matrix,²⁹ semistochastic heat-bath CI,³⁰ adaptive sampling CI,³¹ other variants of selected CI,^{32–34} and many others (see also the references in a recent comprehensive benchmark study³⁵).

Quantum Algorithms for Ab initio Electronic Structure Calculations: Quantum computing (QC) algorithms for AB INITIO electronic structure calculations of quantum chemical research have been intensively surveyed by the review articles 5–10. The iterative QPE scheme proposed by Aspuru-Guzik *et al.*³⁶ and Dobšíček *et al.*³⁷ is the earliest chemical QC algorithm developed along a line of the approach to physical Hamiltonians developed by Abrams and Lloyd.^{38–40} The QPE of Kitaev¹ and Cleve *et al.*⁴¹ allows to extract eigenvalues of the Hamiltonian H from the unitary operator $e^{iH\tau}$ as phases with a binary representation. This QPE-based eigensolver requires circuits with a large number of gates due to a relatively long-time Hamiltonian evolution; thus, its use on the near-term QCs or noisy intermediate-scale quantum (NISQ) devices is considered to be infeasible. The variational quantum eigensolver (VQE)⁴² is a hybrid quantum-classical approach amenable to the NISQ devices. Various wave function ansatze for the state preparation for VQE have been developed and cannot be all cited, but the most extensively studied is the unitary coupled-cluster (UCC) framework, entailing UCC singles and doubles (UCCSD),⁴² generalized UCC singles and doubles (UCCGSD),⁴³ orbital optimized UCC (OO-UCC),⁴⁴ etc. The recently highlighted alternative is the VQE scheme with the adaptive state preparation, including adaptive derivative-assembled pseudo-Trotter (ADAPT),⁴⁵ iterative qubit CC (iQCC),⁴⁶ quantum Monte Carlo (QMC),⁴⁷ etc.⁴⁸

S2 Benchmark Data

S2.1 PECs of H₂ with BM2(FS), BM3(FS), and RBM(FS)

Table S1: Total energies (in E_h) of the H₂ molecule with the bond length r (in Å) calculated with the BM2(FS) model with CAS(2e,2o), STO-3G basis. The various numbers of the energy register qubits are used along with the two types of molecular orbitals, CMO and LMO.

r	CMO					LMO					
	6bit	8bit	10bit	12bit	50bit	6bit	8bit	10bit	12bit	50bit	
0.25	-0.312267	-0.312263	-0.312270	-0.312270	-0.312270	-0.305000	-0.312211	-0.312208	-0.312270	-0.312270	
0.3	-0.601802	-0.601800	-0.601804	-0.601804	-0.601804	-0.593827	-0.601538	-0.601803	-0.601804	-0.601804	
0.35	-0.789091	-0.789269	-0.789269	-0.789269	-0.789269	-0.780454	-0.788657	-0.789228	-0.789269	-0.789269	
0.4	-0.914009	-0.914150	-0.914149	-0.914150	-0.914150	-0.904361	-0.913126	-0.914145	-0.914150	-0.914150	
0.45	-0.998416	-0.998413	-0.998416	-0.998416	-0.998416	-0.989279	-0.998091	-0.998415	-0.998416	-0.998416	
0.5	-1.055009	-1.055154	-1.055160	-1.055160	-1.055160	-1.046371	-1.055107	-1.055158	-1.055159	-1.055160	
0.55	-1.092542	-1.092629	-1.092629	-1.092629	-1.092629	-1.092630	-1.082404	-1.092489	-1.092617	-1.092630	
0.6	-1.116086	-1.116281	-1.116286	-1.116286	-1.116286	-1.109633	-1.115786	-1.116260	-1.116286	-1.116286	
0.65	-1.129905	-1.129902	-1.129905	-1.129905	-1.129905	-1.126546	-1.129886	-1.129904	-1.129905	-1.129905	
0.7	-1.135980	-1.136188	-1.136189	-1.136189	-1.136189	-1.135015	-1.136158	-1.136189	-1.136189	-1.136189	
0.75	-1.136985	-1.137105	-1.137117	-1.137117	-1.137117	-1.137117	-1.136378	-1.137023	-1.137117	-1.137117	
0.8	-1.134102	-1.134147	-1.134148	-1.134148	-1.134148	-1.134048	-1.134003	-1.134144	-1.134148	-1.134148	
0.85	-1.128187	-1.128361	-1.128362	-1.128362	-1.128362	-1.128356	-1.128362	-1.128361	-1.128362	-1.128362	
0.9	-1.120501	-1.120560	-1.120560	-1.120560	-1.120560	-1.120560	-1.120536	-1.120560	-1.120560	-1.120560	
0.95	-1.111303	-1.111339	-1.111339	-1.111339	-1.111339	-1.111186	-1.111324	-1.111338	-1.111339	-1.111339	
1.0	-1.101022	-1.101142	-1.101150	-1.101150	-1.101150	-1.100583	-1.101141	-1.101150	-1.101150	-1.101150	
1.05	-1.090340	-1.090337	-1.090342	-1.090342	-1.090342	-1.090342	-1.090338	-1.090339	-1.090342	-1.090342	
1.1	-1.079144	-1.079193	-1.079193	-1.079193	-1.079193	-1.078489	-1.079176	-1.079192	-1.079193	-1.079193	
1.15	-1.067826	-1.067928	-1.067930	-1.067930	-1.067930	-1.067485	-1.067929	-1.067928	-1.067930	-1.067930	
1.2	-1.056736	-1.056741	-1.056741	-1.056741	-1.056741	-1.056393	-1.056733	-1.056739	-1.056741	-1.056741	
1.25	-1.045632	-1.045768	-1.045783	-1.045783	-1.045783	-1.045783	-1.045615	-1.045741	-1.045776	-1.045783	-1.045783
1.3	-1.033915	-1.035185	-1.035186	-1.035186	-1.035186	-1.035186	-1.035137	-1.035183	-1.035186	-1.035186	-1.035186
1.35	-1.024999	-1.025037	-1.025054	-1.025054	-1.025054	-1.025054	-1.025027	-1.024973	-1.025054	-1.025054	-1.025054
1.4	-1.015137	-1.015439	-1.015468	-1.015468	-1.015468	-1.015468	-1.015466	-1.015466	-1.015468	-1.015468	-1.015468
1.45	-1.006469	-1.006486	-1.006486	-1.006486	-1.006486	-1.006487	-1.006484	-1.006468	-1.006486	-1.006487	-1.006487
1.5	-0.998138	-0.998134	-0.998149	-0.998149	-0.998149	-0.998149	-0.997658	-0.998149	-0.998149	-0.998149	-0.998149
1.55	-0.990179	-0.990456	-0.990476	-0.990476	-0.990476	-0.990476	-0.989855	-0.990469	-0.990476	-0.990476	-0.990476
1.6	-0.982598	-0.983427	-0.983471	-0.983471	-0.983471	-0.983473	-0.983115	-0.983472	-0.983472	-0.983473	-0.983473
1.65	-0.976844	-0.977116	-0.977129	-0.977129	-0.977129	-0.977130	-0.977026	-0.977124	-0.977129	-0.977130	-0.977130
1.7	-0.970808	-0.971412	-0.971427	-0.971427	-0.971427	-0.971427	-0.971377	-0.971420	-0.971427	-0.971427	-0.971427
1.75	-0.965627	-0.966330	-0.966332	-0.966334	-0.966335	-0.966334	-0.966332	-0.966334	-0.966334	-0.966335	-0.966335
1.8	-0.961733	-0.961811	-0.961817	-0.961817	-0.961817	-0.961806	-0.961816	-0.961817	-0.961817	-0.961817	-0.961817
1.85	-0.957829	-0.957833	-0.957832	-0.957832	-0.957832	-0.957833	-0.957818	-0.957832	-0.957833	-0.957833	-0.957833
1.9	-0.954247	-0.954338	-0.954339	-0.954339	-0.954339	-0.954339	-0.953963	-0.954339	-0.954339	-0.954339	-0.954339
1.95	-0.951287	-0.951284	-0.951289	-0.951289	-0.951290	-0.951119	-0.951289	-0.951290	-0.951290	-0.951290	-0.951290

Table S2: Total energies (in E_h) of the H_2 molecule with the bond length r (in Å) calculated with the BM3(FS) model with CAS(2e,2o), STO-3G basis. The various numbers of the energy register qubits are used along with the two types of molecular orbitals, CMO and LMO.

r	CMO					LMO				
	6bit	8bit	10bit	12bit	50bit	6bit	8bit	10bit	12bit	50bit
0.25	-0.312268	-0.312268	-0.312268	-0.312268	-0.312270	-0.305001	-0.305001	-0.312249	-0.312249	-0.312270
0.3	-0.601803	-0.601802	-0.601802	-0.601802	-0.601804	-0.593828	-0.597121	-0.601729	-0.601804	-0.601804
0.35	-0.789268	-0.789268	-0.789267	-0.789268	-0.789269	-0.780455	-0.785193	-0.789071	-0.789254	-0.789269
0.4	-0.914127	-0.914148	-0.914148	-0.914148	-0.914150	-0.904361	-0.910649	-0.913804	-0.914150	-0.914150
0.45	-0.998407	-0.998414	-0.998414	-0.998414	-0.998416	-0.987513	-0.995819	-0.998246	-0.998410	-0.998416
0.5	-1.055128	-1.055158	-1.055159	-1.055159	-1.055160	-1.042996	-1.053442	-1.055151	-1.055139	-1.055160
0.55	-1.092629	-1.092629	-1.092628	-1.092629	-1.092630	-1.079051	-1.091640	-1.092611	-1.092615	-1.092630
0.6	-1.116189	-1.116285	-1.116285	-1.116285	-1.116286	-1.101128	-1.115677	-1.116115	-1.116269	-1.116286
0.65	-1.129902	-1.129903	-1.129904	-1.129905	-1.129905	-1.112997	-1.129667	-1.129644	-1.129903	-1.129905
0.7	-1.135591	-1.136188	-1.136189	-1.136189	-1.136189	-1.117349	-1.136094	-1.135921	-1.136178	-1.136189
0.75	-1.137115	-1.137117	-1.137117	-1.137117	-1.137117	-1.131315	-1.136929	-1.136957	-1.137115	-1.137117
0.8	-1.134147	-1.134148	-1.134147	-1.134148	-1.134148	-1.118071	-1.134148	-1.134147	-1.134148	-1.134148
0.85	-1.128332	-1.128349	-1.128360	-1.128362	-1.128362	-1.123749	-1.128337	-1.128292	-1.128362	-1.128362
0.9	-1.119686	-1.120512	-1.120560	-1.120560	-1.120560	-1.118110	-1.120200	-1.120560	-1.120560	-1.120560
0.95	-1.111021	-1.111310	-1.111336	-1.111339	-1.111339	-1.109683	-1.110476	-1.111326	-1.111338	-1.111339
1.0	-1.101021	-1.101148	-1.101148	-1.101150	-1.101150	-1.084876	-1.100159	-1.101150	-1.101150	-1.101150
1.05	-1.090055	-1.090341	-1.090342	-1.090342	-1.090342	-1.088498	-1.088484	-1.090342	-1.090342	-1.090342
1.1	-1.079006	-1.079179	-1.079193	-1.079193	-1.079193	-1.076560	-1.078486	-1.079189	-1.079193	-1.079193
1.15	-1.067694	-1.067930	-1.067930	-1.067930	-1.067930	-1.065505	-1.067930	-1.067930	-1.067930	-1.067930
1.2	-1.056581	-1.056740	-1.056741	-1.056741	-1.056741	-1.054826	-1.056741	-1.056741	-1.056741	-1.056741
1.25	-1.045394	-1.045754	-1.045783	-1.045783	-1.045783	-1.043210	-1.045783	-1.045783	-1.045783	-1.045783
1.3	-1.035153	-1.035186	-1.035186	-1.035186	-1.035186	-1.029779	-1.035186	-1.035186	-1.035186	-1.035186
1.35	-1.025010	-1.025052	-1.025054	-1.025054	-1.025054	-1.022154	-1.025054	-1.025054	-1.025054	-1.025054
1.4	-1.014970	-1.015464	-1.015468	-1.015468	-1.015468	-1.011621	-1.015465	-1.015468	-1.015468	-1.015468
1.45	-1.005662	-1.006487	-1.006487	-1.006487	-1.006487	-1.005426	-1.006486	-1.006487	-1.006487	-1.006487
1.5	-0.995623	-0.998131	-0.998149	-0.998149	-0.998149	-0.997800	-0.998149	-0.998149	-0.998149	-0.998149
1.55	-0.987852	-0.990441	-0.990476	-0.990476	-0.990476	-0.990362	-0.990476	-0.990476	-0.990476	-0.990476
1.6	-0.982361	-0.983462	-0.983473	-0.983473	-0.983473	-0.983429	-0.983473	-0.983473	-0.983473	-0.983473
1.65	-0.976990	-0.977109	-0.977129	-0.977130	-0.977130	-0.976968	-0.977130	-0.977130	-0.977130	-0.977130
1.7	-0.971427	-0.971427	-0.971426	-0.971427	-0.971427	-0.971415	-0.971426	-0.971427	-0.971427	-0.971427
1.75	-0.966202	-0.966312	-0.966334	-0.966335	-0.966335	-0.966313	-0.966335	-0.966335	-0.966335	-0.966335
1.8	-0.959760	-0.961816	-0.961817	-0.961817	-0.961817	-0.961786	-0.961815	-0.961817	-0.961817	-0.961817
1.85	-0.954561	-0.957814	-0.957833	-0.957833	-0.957833	-0.957816	-0.957798	-0.957833	-0.957833	-0.957833
1.9	-0.954339	-0.954307	-0.954339	-0.954339	-0.954339	-0.954222	-0.954269	-0.954339	-0.954339	-0.954339
1.95	-0.949912	-0.951288	-0.951290	-0.951290	-0.951290	-0.951285	-0.951289	-0.951290	-0.951290	-0.951290

Table S3: Total energies (in E_h) of the H_2 molecule with the bond length r (in Å) calculated with the RBM(FS) model with CAS(2e,2o), STO-3G basis, and 8 energy register qubits. The various numbers of hidden nodes (m) are used along with the two types of molecular orbitals, CMO and LMO.

r	CMO				LMO			
	m=2	m=3	m=4	m=5	m=2	m=3	m=4	m=5
0.25	-0.312259	-0.312260	-0.312246	-0.312254	-0.312083	-0.311148	-0.308093	-0.308011
0.5	-1.055159	-1.055160	-1.055137	-1.055042	-1.053648	-1.052367	-1.055098	-1.050520
0.75	-1.136981	-1.137070	-1.137055	-1.137117	-1.135531	-1.134233	-1.136509	-1.135135
1.0	-1.101049	-1.100949	-1.100875	-1.101148	-1.100870	-1.099773	-1.100024	-1.099571
1.25	-1.045729	-1.045756	-1.045548	-1.045530	-1.044844	-1.044306	-1.045619	-1.044810
1.5	-0.997624	-0.997735	-0.997763	-0.997691	-0.998075	-0.997555	-0.997711	-0.998139
1.75	-0.938459	-0.962518	-0.961720	-0.965965	-0.966151	-0.961567	-0.966172	-0.966239
1.9	-0.925270	-0.950512	-0.946421	-0.953033	-0.931760	-0.951710	-0.954030	-0.953835

Table S4: Total energies (in E_h) of the H_2 molecule with the bond length r (in Å) calculated with the RBM(FS) model with CAS(2e,2o), STO-3G basis, and 50 energy register qubits. The various numbers of hidden nodes (m) are used along with the two types of molecular orbitals, CMO and LMO.

r	CMO				LMO			
	m=2	m=3	m=4	m=5	m=2	m=3	m=4	m=5
0.25	-0.312270	-0.312270	-0.312270	-0.312270	-0.312270	-0.312270	-0.312270	-0.312270
0.5	-1.055160	-1.055160	-1.055160	-1.055160	-1.055160	-1.055160	-1.055160	-1.055160
0.75	-1.137117	-1.137117	-1.137117	-1.137117	-1.137117	-1.137117	-1.137117	-1.137117
1.0	-1.101150	-1.101150	-1.101150	-1.101150	-1.101150	-1.101150	-1.101150	-1.101150
1.25	-1.045783	-1.045783	-1.045783	-1.045783	-1.045783	-1.045783	-1.045783	-1.045783
1.5	-0.998149	-0.998149	-0.998149	-0.998149	-0.998149	-0.998149	-0.998149	-0.998149
1.75	-0.966335	-0.966335	-0.966335	-0.966335	-0.966335	-0.966335	-0.966335	-0.966335
1.9	-0.954339	-0.954339	-0.954339	-0.954339	-0.954339	-0.954339	-0.954339	-0.954339

S2.2 PECs of H₂ with BM2(PN), BM3(PN)

Table S5: Total energies (in E_h) of the H₂ molecule with the bond length r (in Å) calculated with the BM2(PN) model with CAS(2e,2o), STO-3G basis. The various numbers of the energy register qubits are used along with the two types of molecular orbitals, CMO and LMO.

r	CMO					LMO				
	6bit	8bit	10bit	12bit	50bit	6bit	8bit	10bit	12bit	50bit
0.25	-0.312270	-0.312269	-0.312270	-0.312270	-0.312270	-0.312260	-0.312262	-0.312270	-0.312270	-0.312270
0.3	-0.601804	-0.601802	-0.601804			-0.601800	-0.601801	-0.601804		-0.601804
0.35	-0.789250	-0.789268	-0.789269			-0.789268	-0.789269	-0.789269		-0.789269
0.4	-0.914150	-0.914150	-0.914150			-0.914150	-0.914149	-0.914146	-0.914150	
0.45	-0.998416	-0.998415	-0.998416			-0.998416	-0.998376	-0.998415	-0.998416	
0.5	-1.055104	-1.055160	-1.055160	-1.055160	-1.055160	-1.055094	-1.055157	-1.055160	-1.055160	-1.055160
0.55	-1.092591	-1.092630	-1.092630			-1.092630	-1.092603	-1.092629	-1.092630	
0.6	-1.116269	-1.116286	-1.116286			-1.116286	-1.116277	-1.116284	-1.116286	
0.65	-1.129901	-1.129904	-1.129905			-1.129905	-1.129902	-1.129904	-1.129905	
0.7	-1.136153	-1.136189	-1.136189			-1.136189	-1.136188	-1.136189	-1.136189	
0.75	-1.137089	-1.137117	-1.137117	-1.137117	-1.137117	-1.137117	-1.137116	-1.137117	-1.137117	-1.137117
0.8	-1.134148	-1.134147	-1.134148			-1.134148	-1.134138	-1.134147	-1.134148	
0.85	-1.128362	-1.128362	-1.128362			-1.128362	-1.128359	-1.128362		-1.128362
0.9	-1.120552	-1.120559	-1.120560			-1.120560	-1.120559	-1.120560		-1.120560
0.95	-1.111339	-1.111339	-1.111339			-1.111339	-1.111339	-1.111339		-1.111339
1.0	-1.101150	-1.101150	-1.101150	-1.101150	-1.101150	-1.101146	-1.101150	-1.101150	-1.101150	-1.101150
1.05	-1.090342	-1.090342	-1.090342			-1.090342	-1.090341	-1.090341	-1.090342	
1.1	-1.079193	-1.079193	-1.079193			-1.079193	-1.079192	-1.079193		-1.079193
1.15	-1.067929	-1.067930	-1.067930			-1.067930	-1.067929	-1.067929		-1.067930
1.2	-1.056582	-1.056741	-1.056741			-1.056741	-1.056740	-1.056741		-1.056741
1.25	-1.045768	-1.045783	-1.045783	-1.045783	-1.045783	-1.045783	-1.045783	-1.045783	-1.045783	
1.3	-1.035183	-1.035186	-1.035186			-1.035186	-1.035186	-1.035186		-1.035186
1.35	-1.025054	-1.025054	-1.025054			-1.025054	-1.025053	-1.025054		-1.025054
1.4	-1.015468	-1.015468	-1.015468			-1.015468	-1.015468	-1.015468		-1.015468
1.45	-1.006487	-1.006487	-1.006487			-1.006487	-1.006487	-1.006487		-1.006487
1.5	-0.998147	-0.998149	-0.998149	-0.998149	-0.998149	-0.998149	-0.998149	-0.998149	-0.998149	-0.998149
1.55	-0.990475	-0.990476	-0.990476			-0.990476	-0.990476	-0.990476		-0.990476
1.6	-0.983469	-0.983473	-0.983473			-0.983473	-0.983472	-0.983469		-0.983473
1.65	-0.977127	-0.977130	-0.977130			-0.977130	-0.977129	-0.977120		-0.977130
1.7	-0.971416	-0.971427	-0.971427			-0.971427	-0.971426	-0.971398	-0.971427	
1.75	-0.966326	-0.966335	-0.966335	-0.966335	-0.966335	-0.966335	-0.966333	-0.966272	-0.966335	-0.966335
1.8	-0.961817	-0.961817	-0.961817			-0.961817	-0.961813	-0.961685	-0.961817	
1.85	-0.957833	-0.957833	-0.957833			-0.957833	-0.957819	-0.957583	-0.957833	
1.9	-0.954339	-0.954339	-0.954339	-0.954339	-0.954339	-0.954339	-0.954300	-0.953914	-0.954339	-0.954339
1.95	-0.951289	-0.951290	-0.951290			-0.951290	-0.951215	-0.950633	-0.951290	

Table S6: Total energies (in E_h) of the H_2 molecule with the bond length r (in Å) calculated with the BM3(PN) model with CAS(2e,2o), STO-3G basis. The various numbers of the energy register qubits are used along with the two types of molecular orbitals, CMO and LMO.

r	CMO					LMO				
	6bit	8bit	10bit	12bit	50bit	6bit	8bit	10bit	12bit	50bit
0.25	-0.312263	-0.312269	-0.312270	-0.312270	-0.312270	-0.312260	-0.312270	-0.312270	-0.312270	-0.312270
0.3	-0.601802	-0.601802	-0.601804	-0.601804	-0.601804	-0.601800	-0.601804	-0.601804	-0.601804	-0.601804
0.35	-0.789268	-0.789268	-0.789269	-0.789269	-0.789269	-0.789267	-0.789269	-0.789269	-0.789269	-0.789269
0.4	-0.914148	-0.914148	-0.914150	-0.914150	-0.914150	-0.914149	-0.914150	-0.914150	-0.914150	-0.914150
0.45	-0.998414	-0.998414	-0.998416	-0.998416	-0.998416	-0.998415	-0.998416	-0.998416	-0.998416	-0.998416
0.5	-1.055148	-1.055159	-1.055160	-1.055160	-1.055160	-1.055160	-1.055160	-1.055160	-1.055160	-1.055160
0.55	-1.092624	-1.092629	-1.092630	-1.092630	-1.092630	-1.092630	-1.092630	-1.092630	-1.092630	-1.092630
0.6	-1.116286	-1.116286	-1.116286	-1.116286	-1.116286	-1.116286	-1.116286	-1.116286	-1.116286	-1.116286
0.65	-1.129898	-1.129904	-1.129905	-1.129905	-1.129905	-1.129905	-1.129905	-1.129905	-1.129905	-1.129905
0.7	-1.136188	-1.136188	-1.136189	-1.136189	-1.136189	-1.136189	-1.136189	-1.136189	-1.136189	-1.136189
0.75	-1.137093	-1.137116	-1.137117	-1.137117	-1.137117	-1.137117	-1.137117	-1.137117	-1.137117	-1.137117
0.8	-1.134148	-1.134145	-1.134148	-1.134148	-1.134148	-1.134148	-1.134147	-1.134148	-1.134148	-1.134148
0.85	-1.128323	-1.128362	-1.128362	-1.128362	-1.128362	-1.128362	-1.128362	-1.128362	-1.128362	-1.128362
0.9	-1.120560	-1.120560	-1.120560	-1.120560	-1.120560	-1.120560	-1.120560	-1.120560	-1.120560	-1.120560
0.95	-1.111339	-1.111336	-1.111339	-1.111339	-1.111339	-1.111339	-1.111339	-1.111339	-1.111339	-1.111339
1.0	-1.101150	-1.101150	-1.101150	-1.101150	-1.101150	-1.101150	-1.101150	-1.101150	-1.101150	-1.101150
1.05	-1.090328	-1.090342	-1.090342	-1.090342	-1.090342	-1.090342	-1.090342	-1.090342	-1.090342	-1.090342
1.1	-1.079192	-1.079193	-1.079193	-1.079193	-1.079193	-1.079193	-1.079193	-1.079193	-1.079193	-1.079193
1.15	-1.067930	-1.067929	-1.067930	-1.067930	-1.067930	-1.067930	-1.067930	-1.067930	-1.067930	-1.067930
1.2	-1.056741	-1.056741	-1.056741	-1.056741	-1.056741	-1.056741	-1.056741	-1.056741	-1.056741	-1.056741
1.25	-1.045783	-1.045783	-1.045783	-1.045783	-1.045783	-1.045783	-1.045783	-1.045783	-1.045783	-1.045783
1.3	-1.035184	-1.035186	-1.035186	-1.035186	-1.035186	-1.035186	-1.035186	-1.035186	-1.035186	-1.035186
1.35	-1.025054	-1.025054	-1.025054	-1.025054	-1.025054	-1.025054	-1.025054	-1.025054	-1.025054	-1.025054
1.4	-1.015460	-1.015468	-1.015468	-1.015468	-1.015468	-1.015468	-1.015468	-1.015468	-1.015468	-1.015468
1.45	-1.006487	-1.006487	-1.006487	-1.006487	-1.006487	-1.006487	-1.006487	-1.006487	-1.006487	-1.006487
1.5	-0.998149	-0.998149	-0.998149	-0.998149	-0.998149	-0.998149	-0.998149	-0.998149	-0.998149	-0.998149
1.55	-0.990476	-0.990476	-0.990476	-0.990476	-0.990476	-0.990476	-0.990476	-0.990476	-0.990476	-0.990476
1.6	-0.983469	-0.983473	-0.983473	-0.983473	-0.983473	-0.983473	-0.983473	-0.983473	-0.983473	-0.983473
1.65	-0.977128	-0.977130	-0.977130	-0.977130	-0.977130	-0.977130	-0.977130	-0.977130	-0.977130	-0.977130
1.7	-0.971427	-0.971427	-0.971427	-0.971427	-0.971427	-0.971427	-0.971427	-0.971427	-0.971427	-0.971427
1.75	-0.966333	-0.966334	-0.966335	-0.966335	-0.966335	-0.966335	-0.966335	-0.966335	-0.966335	-0.966335
1.8	-0.961817	-0.961817	-0.961817	-0.961817	-0.961817	-0.961817	-0.961817	-0.961817	-0.961817	-0.961817
1.85	-0.957832	-0.957833	-0.957833	-0.957833	-0.957833	-0.957833	-0.957833	-0.957833	-0.957833	-0.957833
1.9	-0.954334	-0.954339	-0.954339	-0.954339	-0.954339	-0.954339	-0.954339	-0.954339	-0.954339	-0.954339
1.95	-0.951290	-0.951289	-0.951289	-0.951289	-0.951289	-0.951289	-0.951289	-0.951289	-0.951289	-0.951289

S2.3 *s-trans* and *s-cis* butadiene with BM2(FS), BM3(FS), and RBM(FS)

Table S7: Total energies (in E_h) of the *s-trans* and *s-cis* isomers obtained with the BM2(FS), BM3(FS), and RBM(FS) calculations using STO-3G basis with CAS(4e,4o). The various numbers of the energy register qubits are used along with the two types of molecular orbitals, CMO and LMO. For comparison, the Hartree-Fock and CAS-CI energies are included.

	<i>s-trans</i> CMO	<i>s-cis</i> CMO	diff(E_h)	<i>s-trans</i> LMO	<i>s-cis</i> LMO	diff(E_h)
Hartree Fock	-153.016495	-153.014039	0.002455			
CAS-CI(4e4o)	-153.102700	-153.100302	0.002397	-153.102700	-153.100302	0.002397
BM2(6bit)	-153.077947	-153.050326	0.027621	-153.052209	-153.071528	-0.019319
BM2(8bit)	-153.089587	-153.088317	0.001270	-153.100664	-153.096572	0.004092
BM2(10bit)	-153.089935	-153.088592	0.001343	-153.102479	-153.100130	0.002349
BM2(12bit)	-153.089951	-153.088612	0.001339	-153.102664	-153.100259	0.002405
BM2(fullbit)	-153.089953	-153.088615	0.001338	-153.102669	-153.100263	0.002407
BM3(6bit)	-153.051866	-153.050821	0.001045	-152.985678	-152.994136	-0.008458
BM3(8bit)	-153.093081	-153.090682	0.002399	-153.093450	-153.091787	0.001663
BM3(10bit)	-153.095782	-153.092748	0.003034	-153.101713	-153.099421	0.002292
BM3(12bit)	-153.095867	-153.092938	0.002929	-153.102331	-153.099962	0.002369
BM3(fullbit)	-153.096019	-153.093010	0.003009	-153.102689	-153.100298	0.002391
RBM(8bit) $n_h = 4$	-153.026099	-153.028396	-0.002297	-152.791247	-152.792737	-0.001490

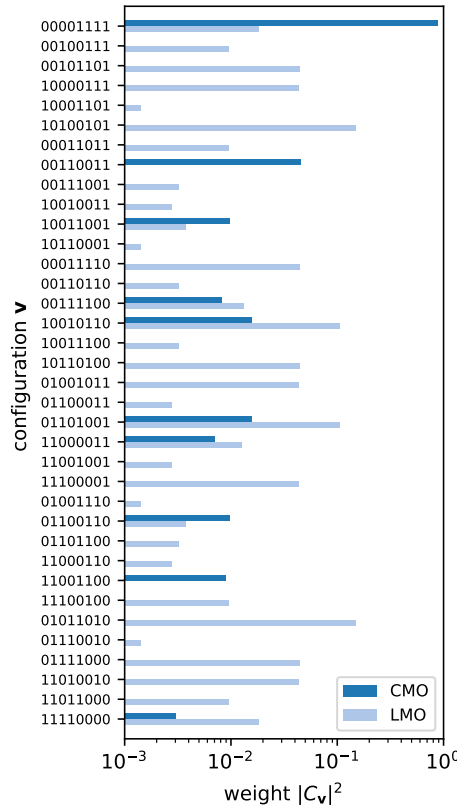


Figure S2: Configuration weights for *s-trans* butadiene calculated at CAS-CI level of theory with CMO and LMO basis.

S2.4 PECs of PABI with BM2(PN) and BM3(PN)

Table S8: Total energies (in E_h) of PABI along the ring-opening reaction coordinate, obtained with the BM2(PN) and BM3(PN) calculations using STO-3G basis with CAS(4e,4o). The progress of the reaction is indexed by an integer number. The various numbers of the energy register qubits are used along with the two types of molecular orbitals, CMO and LMO. For comparison, the Hartree-Fock and CAS-CI energies are included.

index	BM2				BM3			
	CMO		LMO		CMO		LMO	
	6bit	50bit	6bit	50bit	6bit	50bit	6bit	50bit
0	-1575.460051	-1575.460081	-1575.459121	-1575.460079	-1575.460080	-1575.460081	-1575.459162	-1575.460082
1	-1575.462243	-1575.462275	-1575.460747	-1575.462275	-1575.462268	-1575.462275	-1575.461207	-1575.462275
2	-1575.457646	-1575.457666	-1575.456920	-1575.457662	-1575.457638	-1575.457655	-1575.456899	-1575.457666
4	-1575.422039	-1575.422046	-1575.421903	-1575.422030	-1575.422044	-1575.422043	-1575.421838	-1575.422047
6	-1575.372116	-1575.372118	-1575.372087	-1575.372111	-1575.372112	-1575.372111	-1575.372055	-1575.372116
8	-1575.322920	-1575.322937	-1575.322681	-1575.322875	-1575.322886	-1575.322936	-1575.322896	-1575.322944
10	-1575.330801	-1575.330809	-1575.330643	-1575.330782	-1575.330174	-1575.330932	-1575.330696	-1575.330931
12	-1575.338117	-1575.338229	-1575.337541	-1575.337577	-1575.338060	-1575.338255	-1575.337691	-1575.338243
14	-1575.342082	-1575.342104	-1575.342003	-1575.342085	-1575.342033	-1575.342095	-1575.342044	-1575.342097
16	-1575.342905	-1575.342941	-1575.342802	-1575.342928	-1575.342669	-1575.342945	-1575.342648	-1575.342950
18	-1575.343557	-1575.343595	-1575.343435	-1575.343564	-1575.343095	-1575.343599	-1575.343423	-1575.343606

S2.5 LMOs used in the calculation for PABI

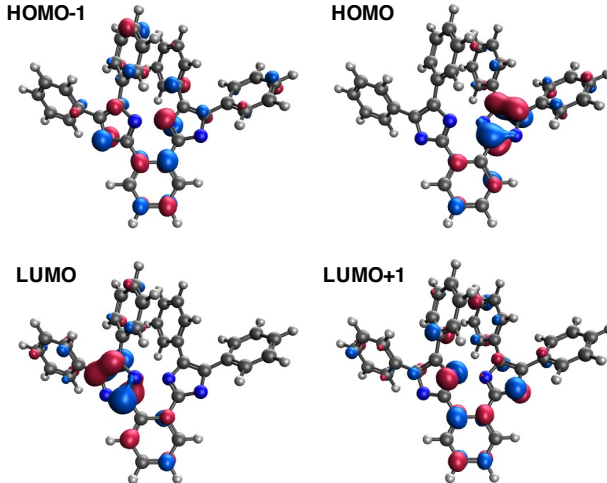


Figure S3: LMOs used as active orbitals for the reaction coordinate index 18.

S2.6 Configuration weights for PABI

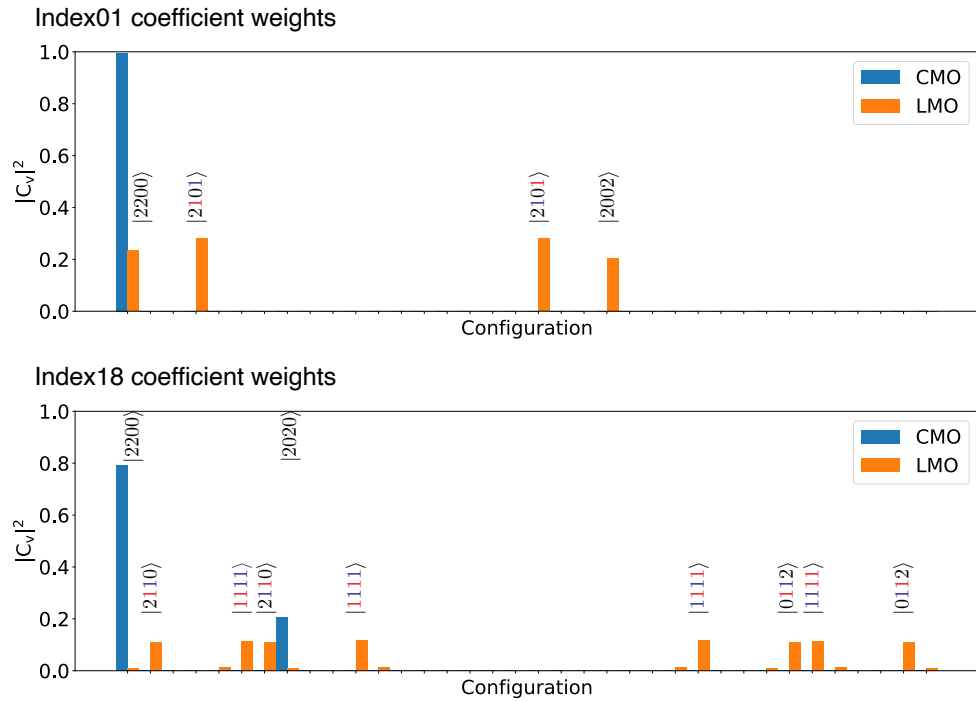


Figure S4: Configuration weights for PABI determined at CAS-CI level of theory using CMO and LMO basis with the reaction coordinate indices 01 and 18.

References

- (1) Kitaev, A. Y. Quantum measurements and the Abelian stabilizer problem. *arXiv preprint quant-ph/9511026* **1995**,
- (2) Brassard, G.; Hoyer, P.; Mosca, M.; Tapp, A. Quantum amplitude amplification and estimation. *Contemporary Mathematics* **2002**, *305*, 53–74.
- (3) Gard, B. T.; Zhu, L.; Barron, G. S.; Mayhall, N. J.; Economou, S. E.; Barnes, E. Efficient symmetry-preserving state preparation circuits for the variational quantum eigensolver algorithm. *npj Quantum Inf.* **2020**, *6*, 1–9.
- (4) Yang, P.-J.; Sugiyama, M.; Tsuda, K.; Yanai, T. Artificial Neural Networks Applied as Molecular Wave Function Solvers. *J. Chem. Theory Comput.* **2020**, *16*, 3513–3529.
- (5) Cao, Y.; Romero, J.; Olson, J. P.; Degroote, M.; Johnson, P. D.; Kieferová, M.; Kivlichan, I. D.; Menke, T.; Peropadre, B.; Sawaya, N. P. D.; Sim, S.; Veis, L.; Aspuru-Guzik, A. Quantum Chemistry in the Age of Quantum Computing. *Chem. Rev.* **2019**, *119*, 10856–10915.
- (6) McArdle, S.; Endo, S.; Aspuru-Guzik, A.; Benjamin, S. C.; Yuan, X. Quantum computational chemistry. *Rev. Mod. Phys.* **2020**, *92*, 015003.
- (7) Bauer, B.; Bravyi, S.; Motta, M.; Chan, G. K.-L. Quantum Algorithms for Quantum Chemistry and Quantum Materials Science. *Chem. Rev.* **2020**, *120*, 12685–12717.
- (8) Bharti, K.; Cervera-Lierta, A.; Kyaw, T. H.; Haug, T.; Alperin-Lea, S.; Anand, A.; Degroote, M.; Heimonen, H.; Kottmann, J. S.; Menke, T.; Mok, W.-K.; Sim, S.; Kwek, L.-C.; Aspuru-Guzik, A. Noisy intermediate-scale quantum algorithms. *Rev. Mod. Phys.* **2022**, *94*, 015004.
- (9) Tilly, J.; Chen, H.; Cao, S.; Picozzi, D.; Setia, K.; Li, Y.; Grant, E.; Wossnig, L.; Rungger, I.; Booth, G. H., et al. The Variational Quantum Eigensolver: a review of methods and best practices. *arXiv preprint arXiv:2111.05176* **2021**,
- (10) Anand, A.; Schleich, P.; Alperin-Lea, S.; Jensen, P. W. K.; Sim, S.; Díaz-Tinoco, M.; Kottmann, J. S.; Degroote, M.; Izmaylov, A. F.; Aspuru-Guzik, A. A quantum computing view on unitary coupled cluster theory. *Chem. Soc. Rev.* **2022**, *51*, 1659–1684.
- (11) Suzuki, Y. et al. Qulacs: a fast and versatile quantum circuit simulator for research purpose. *Quantum* **2021**, *5*, 559.
- (12) Jordan, P.; Wigner, E. Pauli's equivalence prohibition. *Z. Physik* **1928**, *47*, 631.
- (13) McClean, J. R. et al. OpenFermion: the electronic structure package for quantum computers. *Quantum Sci. Technol.* **2020**, *5*, 034014.
- (14) Sun, Q.; Berkelbach, T. C.; Blunt, N. S.; Booth, G. H.; Guo, S.; Li, Z.; Liu, J.; McClain, J. D.; Sayfutyarova, E. R.; Sharma, S.; Wouters, S.; Chan, G. K.-L. PySCF: the Python-based simulations of chemistry framework. *WIREs Comput. Mol. Sci.* **2018**, *8*, e1340.
- (15) Sorella, S. Generalized Lanczos algorithm for variational quantum Monte Carlo. *Physical Review B* **2001**, *64*, 024512–.
- (16) Orús, R. Tensor networks for complex quantum systems. *Nat. Rev. Phys.* **2019**, *1*, 538–550.
- (17) White, S. R. Density matrix formulation for quantum renormalization groups. *Phys. Rev. Lett.* **1992**, *69*, 2863–2866.
- (18) White, S. R. Density-matrix algorithms for quantum renormalization groups. *Phys. Rev. B* **1993**, *48*, 10345–10356.
- (19) Schollwöck, U. The density-matrix renormalization group in the age of matrix product states. *Ann. Phys.* **2011**, *326*, 96–192.

- (20) Chan, G. K.-L.; Keselman, A.; Nakatani, N.; Li, Z.; White, S. R. Matrix product operators, matrix product states, and ab initio density matrix renormalization group algorithms. *J. Chem. Phys.* **2016**, *145*, 014102.
- (21) Shi, Y.-Y.; Duan, L.-M.; Vidal, G. Classical simulation of quantum many-body systems with a tree tensor network. *Phys. Rev. A* **2006**, *74*, 022320.
- (22) Verstraete, F.; Cirac, J. I. Renormalization algorithms for quantum-many body systems in two and higher dimensions. *arXiv preprint cond-mat/0407066* **2004**,
- (23) Vidal, G. Entanglement Renormalization. *Phys. Rev. Lett.* **2007**, *99*, 220405.
- (24) Chan, G. K.-L.; Sharma, S. The Density Matrix Renormalization Group in Quantum Chemistry. *Annu. Rev. Phys. Chem.* **2011**, *62*, 465–481.
- (25) Booth, G. H.; Thom, A. J. W.; Alavi, A. Fermion Monte Carlo without fixed nodes: A game of life, death, and annihilation in Slater determinant space. *J. Chem. Phys.* **2009**, *131*, 054106.
- (26) Xu, E.; Uejima, M.; Ten-no, S. L. Full Coupled-Cluster Reduction for Accurate Description of Strong Electron Correlation. *Phys. Rev. Lett.* **2018**, *121*, 113001.
- (27) Eriksen, J. J.; Lippurini, F.; Gauss, J. Virtual Orbital Many-Body Expansions: A Possible Route towards the Full Configuration Interaction Limit. *J. Phys. Chem. Lett.* **2017**, *8*, 4633–4639.
- (28) Shi, H.; Zhang, S. Some recent developments in auxiliary-field quantum Monte Carlo for real materials. *J. Chem. Phys.* **2021**, *154*, 024107.
- (29) Fosso-Tande, J.; Nguyen, T.-S.; Gidofalvi, G.; DePrince, A. E. Large-Scale Variational Two-Electron Reduced-Density-Matrix-Driven Complete Active Space Self-Consistent Field Methods. *J. Chem. Theory Comput.* **2016**, *12*, 2260–2271.
- (30) Li, J.; Otten, M.; Holmes, A. A.; Sharma, S.; Umrigar, C. J. Fast semistochastic heat-bath configuration interaction. *J. Chem. Phys.* **2018**, *149*, 214110.
- (31) Levine, D. S.; Hait, D.; Tubman, N. M.; Lehtola, S.; Whaley, K. B.; Head-Gordon, M. CASSCF with Extremely Large Active Spaces Using the Adaptive Sampling Configuration Interaction Method. *J. Phys. Chem. Lett.* **2020**, *16*, 2340–2354.
- (32) Neese, F. A spectroscopy oriented configuration interaction procedure. *J. Chem. Phys.* **2003**, *119*, 9428–9443.
- (33) Schriber, J. B.; Evangelista, F. A. Communication: An adaptive configuration interaction approach for strongly correlated electrons with tunable accuracy. *J. Chem. Phys.* **2016**, *144*, 161106.
- (34) Abraham, V.; Mayhall, N. J. Selected Configuration Interaction in a Basis of Cluster State Tensor Products. *J. Chem. Theory Comput.* **2020**, *16*, 6098–6113.
- (35) Eriksen, J. J. et al. The Ground State Electronic Energy of Benzene. *J. Phys. Chem. Lett.* **2020**, *11*, 8922–8929.
- (36) Aspuru-Guzik, A.; Dutoi, A. D.; Love, P. J.; Head-Gordon, M. Simulated Quantum Computation of Molecular Energies. *Science* **2005**, *309*, 1704–1707.
- (37) Dobšíček, M.; Johansson, G.; Shumeiko, V.; Wendin, G. Arbitrary accuracy iterative quantum phase estimation algorithm using a single ancillary qubit: A two-qubit benchmark. *Phys. Rev. A* **2007**, *76*, 03030.
- (38) Seth, L. Universal Quantum Simulators. *Science* **1996**, *273*, 1073–1078.
- (39) Abrams, D. S.; Lloyd, S. Simulation of Many-Body Fermi Systems on a Universal Quantum Computer. *Phys. Rev. Lett.* **1997**, *79*, 2586–2589.
- (40) Abrams, D. S.; Lloyd, S. Quantum Algorithm Providing Exponential Speed Increase for Finding Eigenvalues and Eigenvectors. *Phys. Rev. Lett.* **1999**, *83*, 5162–5165.
- (41) Cleve, R.; Ekert, A.; Macchiavello, C.; Mosca, M. Quantum algorithms revisited. *Proc. R. Soc. A: Math. Phys. Eng. Sci.* **1998**, *454*, 339–354.

- (42) Peruzzo, A.; McClean, J.; Shadbolt, P.; Yung, M.-H.; Zhou, X.-Q.; Love, P. J.; Aspuru-Guzik, A.; O'Brien, J. L. A variational eigenvalue solver on a photonic quantum processor. *Nat. Commun.* **2014**, *5*, 4213.
- (43) Lee, J.; Huggins, W. J.; Head-Gordon, M.; Whaley, K. B. Generalized Unitary Coupled Cluster Wave functions for Quantum Computation. *J. Chem. Theory Comput.* **2019**, *15*, 311–324.
- (44) Mizukami, W.; Mitarai, K.; Nakagawa, Y. O.; Yamamoto, T.; Yan, T.; Ohnishi, Y.-y. Orbital optimized unitary coupled cluster theory for quantum computer. *Phys. Rev. Res.* **2020**, *2*, 033421–.
- (45) Grimsley, H. R.; Economou, S. E.; Barnes, E.; Mayhall, N. J. An adaptive variational algorithm for exact molecular simulations on a quantum computer. *Nat. Commun.* **2019**, *10*, 3007.
- (46) Ryabinkin, I. G.; Yen, T.-C.; Genin, S. N.; Izmaylov, A. F. Qubit Coupled Cluster Method: A Systematic Approach to Quantum Chemistry on a Quantum Computer. *J. Chem. Theory Comput.* **2018**, *14*, 6317–6326.
- (47) Huggins, W. J.; O’Gorman, B. A.; Rubin, N. C.; Reichman, D. R.; Babbush, R.; Lee, J. Unbiasing fermionic quantum Monte Carlo with a quantum computer. *Nature* **2022**, *603*, 416–420.
- (48) Stair, N. H.; Evangelista, F. A. Simulating Many-Body Systems with a Projective Quantum Eigensolver. *PRX Quantum* **2021**, *2*, 030301–.